DOR: 20.1001.1.2322388.2020.8.4.2.7

Research Paper

Tribological Properties of Al2024-2wt.%TiO_2 Nanocomposite Produced by Mechanical Alloying and Hot-Pressing

Hamid Ashrafi*

Faculty of Chemical and Materials Engineering, Shahrood University of Technology, Shahrood, 3619995161, Iran

ARTICLE INFO

Article history:

Received 26 April 2020
Accepted 6 June 2020
Available online 10 October 2020

Keywords:

Al2024 alloy
Nanocomposite
Hardness
Wear

ABSTRACT

Aluminum matrix composites have recently gained increased attention for structural applications in many industries due to their excellent properties. In this research, machining scraps of coarse-grained Al2024-T3 alloy were used to prepare nanostructured Al2024 alloy and Al2024-2wt.%TiO_2 nanocomposite. Then, tribological behavior of bulk nanostructured Al2024 alloy and Al2024-2wt.%TiO_2 nanocomposite, produced by 10 h of mechanical alloying and subsequent hot-pressing at 500 °C for 20 min, was investigated. Hardness measurements on the samples revealed that the hardness value of mechanically alloyed and hot-pressed Al2024 alloy reached a value of ~ 198 HV, which was ~ 41% higher than that for the initial coarse-grained Al2024-T3 alloy (140 HV). The average hardness values of Al2024-2wt.%TiO_2 nanocomposite was found to be 238 HV, which showed ~ 20% increase compared with that for the nanostructured Al2024 alloy. The wear resistance of samples changed in the order of coarse-grained Al2024 alloy <nanostructured Al2024 alloy <Al2024 2wt.%TiO_2 nanocomposite, where the wear rate of the Al2024-2wt.%TiO_2 nanocomposite was about 0.66 of that for the nanostructured Al2024 alloy. For all samples, the wear took place by a combination of abrasion, adhesion, and delamination mechanisms. A mechanically mixed layer (MML) containing a considerable amount of Fe and O was formed on the worn surface of all samples.

* **Corresponding Author:**
Email Address: hashrafi@shahroodut.ac.ir

1. Introduction

Aluminum matrix composites (AMCs) have allocated considerable attention in the past decades because of their excellent properties such as low coefficient of thermal expansion, high elastic modulus, high specific strength, and increased wear resistance over most conventional materials [1-3]. These properties make AMCs an attractive choice for structural applications in aircraft, automotive and military industries [4, 5]. The fabrication methods to produce particulate reinforced AMCs are mainly divided into two types: solid-state process [6-8] and liquid state [9, 10]. Liquid state techniques (such as casting) have some disadvantages like poor wetting between Al and ceramic particles and the formation of undesirable compounds due to the chemical reactions at high temperatures. These disadvantages make the fabrication of AMCs through casting methods very difficult and degrade the mechanical properties of the composite [11-13]. Powder metallurgy is another approach for the fabrication of AMCs by mixing the powders of the Al alloy with ceramic particles followed by consolidation. Avoiding detrimental interfacial reaction because of a lower manufacturing temperature and the possibility of adding higher amounts of reinforcement particles are advantages of this process [14-16]. In general, mechanical alloying (MA) is often used to prepare AMCs powder. MA is a solid-state processing technique which completely carried out at room temperature [17]. This process can produce metal matrix composite powders with a uniform dispersion of the reinforcement particles in the matrix. In this process, reinforcement particles being well embedded into the matrix particles through a repeated process of cold welding, fracturing, and re-welding [18-21]. MA is also capable of producing nanostructured materials, and as a result, nanostructured composite powders can be obtained using this method [22, 23]. Ceramic particles such as SiC and Al_2O_3 are the most widely used materials as reinforcement in AMCs [24]. TiO_2 is one of the most promising ceramic materials because of its high hardness and elastic modulus, superior corrosion resistance, and good wear behavior [25, 26]. Nevertheless, the use of TiO_2 as reinforcement in aluminum alloys has received little attention. Sivasankaran et al. [27] investigated the sinterability and hardness of Al6061-TiO_2 micro and nanocomposites prepared by high energy ball milling and subsequent cold pressing and sintering. Their results revealed that the hardness of nanocomposites was around 3-4 times higher than that for microcomposites. Bera et al. [28] demonstrated that Al7075-nano TiO_2 composite synthesized by mechanical milling and consolidated by equal channel angular pressing had improved mechanical properties compared with the monolithic Al7075 alloy. Karunanithi et al. [25] showed that Al7075-TiO_2 composites fabricated by powder metallurgy method had better corrosion resistance in comparison with Al7075 alloy. Kumar and Rajadurai [26] investigated the influence of TiO_2 content on wear characteristics of Al-15%SiC composite produced by powder metallurgy. Their results indicated that wear resistance and microhardness increased with the increase of TiO_2 content. Although in recent years, Al2024-TiO_2 nanocomposite has been fabricated by stir casting method [29], no study in the field of preparation and characterization of Al2024-TiO_2 nanocomposite by powder metallurgy can be found in the literature. Therefore, the objective of this study was to prepare a bulk Al-TiO_2 nanocomposite by MA and hot-pressing methods. Then, the wear behavior was investigated under dry sliding conditions and was compared to that for nanostructured and coarse-grained Al2024 alloys. The TiO_2 content (2 wt.%) was selected so that both excessive agglomerations were avoided and full dense samples could be obtained after HP, as high volume fraction of reinforcement in Al matrix composites reduces compressibility and enhances agglomeration of the second phase particles [30, 31].

2. Experimental procedure

The materials used in this study were residual machining scraps of Al2024-T3 bars and nano-sized TiO_2 powder (purity > 99.5 %, US nano). Fig. 1 shows the morphology of the initial materials. The machining scraps had a spring-like morphology. Nano-sized TiO_2 powders were spherical with a mean particle size of ~ 80 nm. The machining scraps were de-greased and washed with acetone before use.

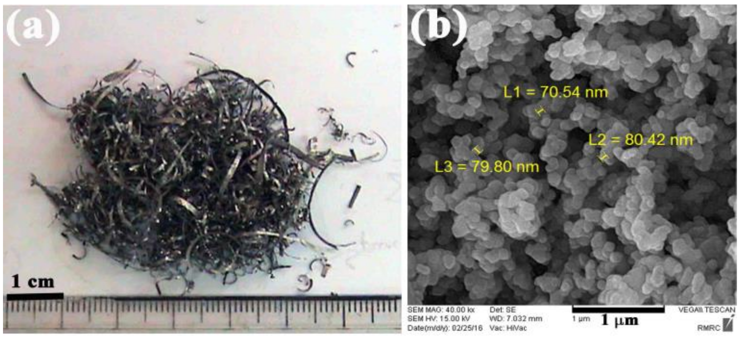

Fig. 1. Morphology of the raw materials, (a) Al2024 scraps, (b) TiO_2 powder.

In order to produce nanostructured Al2024 powder, the scraps were mechanically milled in a high-energy planetary ball mill at room temperature and under argon atmosphere for 10 h. This time was the minimum time that Al2024 powder could be prepared from machining scraps by MA. Possessing parameters of milling are given in Table 1. These parameters are typical for the MA of Al alloys. To prevent sever sticking of Al powders to balls and vial surfaces, 1 wt.% of stearic acid was used as the process control agent (PCA).

Table 1. Processing parameters of MA

Rotation speed of vial (rpm)	500
Rotation speed of disc (rpm)	250
Diameter of vial (mm)	90
Diameter of disc (mm)	350
Vial material	Hardened Cr steel
Capacity of vial (ml)	120
Ball material	Hardened carbon steel
Diameter of balls (mm)	20
Number of balls	5
Ball to powder weight ratio	20:1
Total powder mass (g)	8.5
Atmosphere of MA	Ar

The Al2024 powder obtained through mechanical milling, which from now on referred to as the nanostructured Al2024, was separately blended with 2 wt.% of nano-sized TiO_2 powders and then mechanically milled for an additional 5 h to produce Al2024-2wt.% TiO_2 nanocomposite powder. The time for the second MA operation was selected based on the literature. Similar MA parameters have been employed for the preparation of Al2014-TiC [32], Al-SiC [33], and Al2017-Al_2O_3-SiC [34] composites. The nanocomposite powder and the nanostructured Al2024 powder underwent uniaxial hot-pressing (HP) in hardened steel die made of X40CrMoV51 (AISI H13) at 500 °C under a pressure of 300 MPa for 20 min to produce disks of F50 mm × 15 mm. The heating rate of HP was ~ 100 °C/min, and the hot-pressed samples were cooled in the air. No degassing was performed before HP operations.

The morphology of powder particles after milling as well as the microstructure and elemental mapping of the cross-section of the milled powders were analyzed by scanning electron microscopy (SEM) in a VEGA\TESCAN equipped with energy-dispersive spectroscopy (EDS) analysis at an acceleration voltage of 15 kV. Phase analysis of the bulk samples was determined by X-ray diffraction (XRD) in a Philips X Pert diffractometer using filtered Cu Ka radiation (l = 0.15406 nm). The grain size and internal strain were estimated from the XRD line broadening using the Williamson-Hall method [35]:

$$\beta Cos\theta = \frac{0.9\lambda}{D} + 2\varepsilon Sin\theta \quad (1)$$

where β is the peak width at half maximum intensity, θ is the Bragg angle, λ is the wavelength of the X-ray (0.15406 nm), D is the average grain size, and ε is the mean value of internal strain. The density of the hot-pressed specimens was measured according to the Archimedes method with water as the measuring liquid. Hardness values were determined by Vickers indenter at a load of 10 kg.

Friction and wear properties of the hot-pressed specimens, as well as the initial coarse-grained Al-2024-T3 alloy, were investigated by a pin-on-disk wear test machine according to the ASTM-G99-05 standard [36], where AISI 52100 steel with the hardness value of 63 HRC was used as the pin. The tests were conducted at room temperature and relative humidity of 30% under dry conditions. The sliding speed was 0.11 m/s, and an applied normal load of 15 N was employed. The mass losses of the disks were measured at different time intervals in the sliding distance with an analytical balance of 0.1 mg precision. The friction coefficients were continuously recorded with the sliding distance. The worn surfaces and wear debris were examined by SEM.

3. Results and discussion

3.1. Morphology and microstructure of powders

The morphology of powder particles is one of the most important parameters to affect the consolidation process and thus the properties of the bulk material. Fig. 2 illustrates the morphologies of mechanically milled Al2024 alloy and Al2024-2wt.% nanocomposite. During the MA process, powder particles underwent severe ball collisions and repeated fracturing and cold welding, which lead to particle size reduction [18]. Both powder mixtures showed a nearly equiaxed morphology, but their particle size differed significantly. The smaller particle size of nanocomposite powder was because it underwent a second milling step to disperse the TiO_2 nanoparticles in the Al2024 alloy matrix. By the dispersion of TiO_2 nanoparticles, the powders became more brittle and fractured easily to form smaller particles.

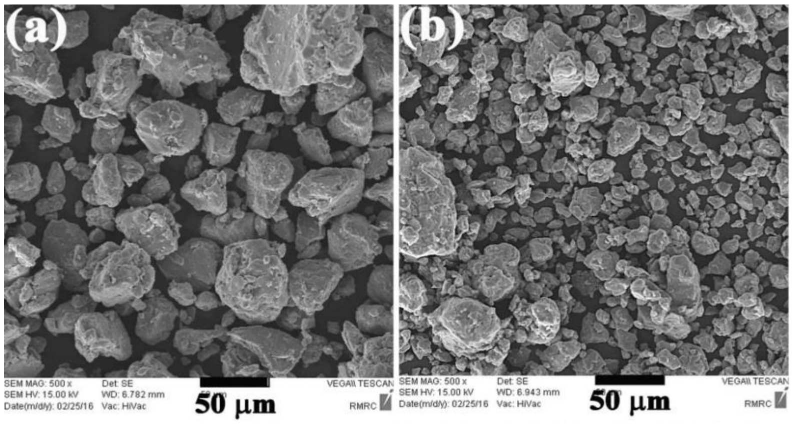

Fig. 2. SEM images of the morphology of the milled powders, (a) Al2024, (b) Al2024-2wt.% TiO_2.

SEM micrograph of the cross-section of the Al2024-2wt.% TiO_2 powder after MA, with the corresponding elemental maps of Al, Ti, and O and also the EDS spectra are shown in Fig. 3. The distribution of Ti and O elements within the Al alloy particles indicates that TiO_2 nanoparticles are well embedded in the Al matrix after MA.

3.2. Phase analysis of powders

The milled powders were hot-pressed at 500 °C under a pressure of 300 MPa for 30 minutes to produce bulk samples. Fig. 4 shows the XRD patterns of the hot-pressed samples. For both samples, only the Al peaks were present. The absence of the TiO_2 peaks can be attributed to its small amount or low diffraction factor. Based on the XRD patterns, the crystallite size and internal strain of Al in the Al2024 alloy and Al2024-2wt.%TiO_2 nanocomposite were calculated by the Williamson-Hall method. The crystallite size of Al in both samples was less than 60 nm (56 and 50 nm), which is typical for the mechanically milled and heat- treated Al alloys [37, 38]. The Al lattice also had a high level of internal strain (> 0.5).

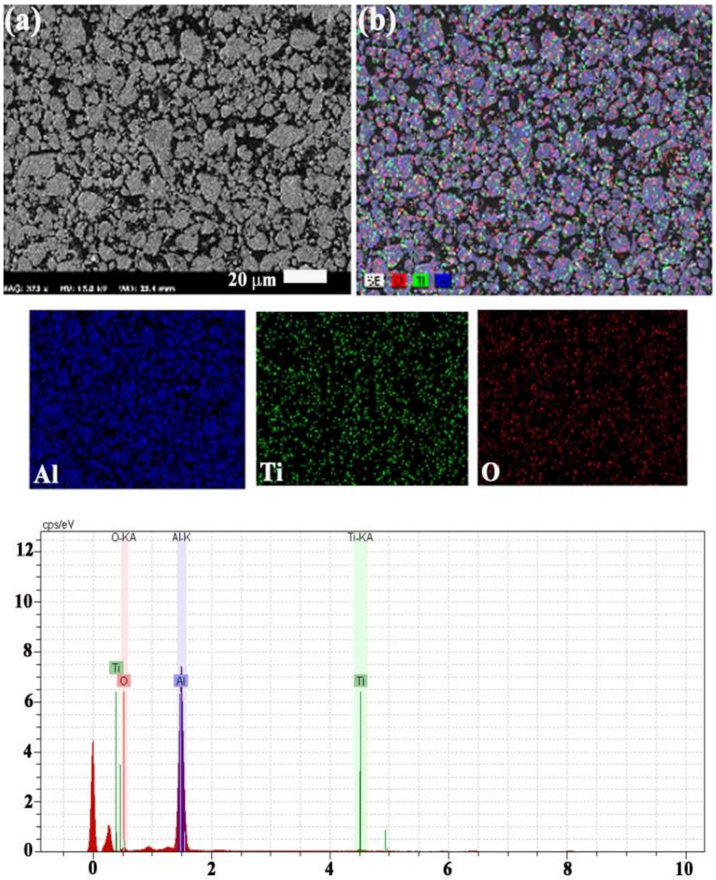

Fig. 3. (a) SEM micrograph of the cross-section of the Al2024-2wt.% TiO_2 powder after MA, with (b) corresponding elemental maps of Al, Ti and O and also the EDS spectra of the powders.

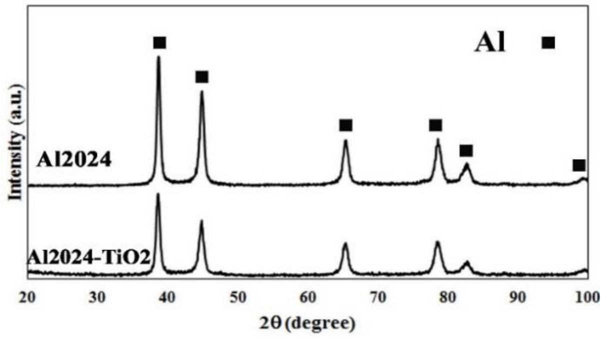

Fig. 4. XRD patterns of the mechanically milled and hot-pressed samples, (a) nanostructured Al2024 alloy, (b) Al2024-2wt.%TiO_2 nanocomposite.

3.3. Density and hardness

The density of the hot-pressed specimens was measured using the Archimedes method. The bulk nanostructured Al2024 alloy showed a high relative density of 99%. A negligible decrease in relative density to 97% occurred with the addition of TiO_2 particles due to the decrease in the compressibility of powders. The hardness of the initial coarse-grained Al2024-T3 alloy, nanostructured Al2024 alloy, and Al2024-2wt.%TiO_2 nanocomposite is shown in Fig. 5. As can be seen, the average hardness value of the bulk nanostructured Al2024 alloy is ~ 198 HV, which is ~ 41% higher than that for the initial coarse-grained Al2024-T3 material (140 HV). This value is also very close to that reported by Jafari et al. [39] for the hardness value of nanostructured Al2024 alloy produced by MA and hot-pressing (206 HV). The average hardness values of Al2024-2wt.%TiO_2 nanocomposite were measured to be 238 HV, which shows ~ 20% improvement compared with the nanostructured Al2024 alloy. The enhanced hardness value of the Al2024-2wt.%TiO_2 nanocomposite compared with the nanostructured Al2024 alloy can be attributed to the presence of very fine and hard particles of TiO_2. According to the strengthening mechanisms, the increase in strength as a result of the presence of a second phase linearly increases with decreasing its particle size [40].

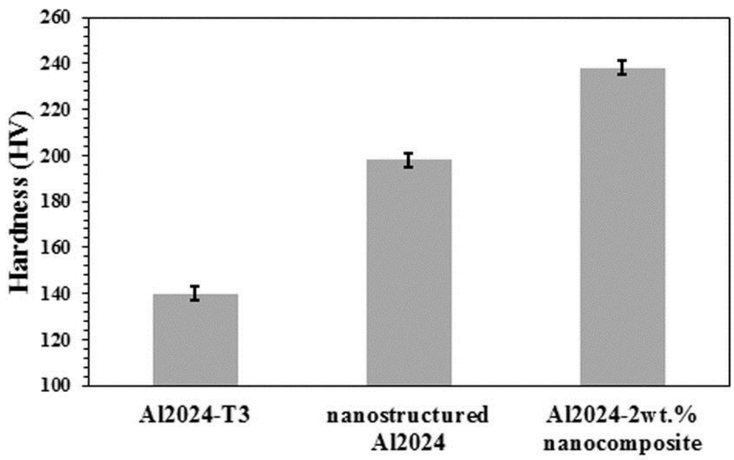

Fig. 5. Bar chart showing the hardness value for the initial coarse-grained Al2024-T3 alloy, nanostructured Al2024 alloy and Al2024-2wt.%TiO_2 nanocomposite prepared by MA and HP.

3.4. Wear behavior

The wear mass losses of the samples as a function of the sliding distance are shown in Fig. 6a. For all samples, the weight loss continuously increased with increasing the sliding distance, but the rate of mass loss decreased at higher sliding distances. Fig. 6b presents the wear rate of samples at the applied normal load of 15 N. The wear resistance of samples changed in the order of coarse-grained Al2024-T3 alloy < nanostructured Al2024 alloy < Al2024 nanocomposite, where the wear rate of Al2024 2wt.%TiO_2 nanocomposite was about 0.66 of that for the nanostructured Al2024 alloy. The higher wear resistance of Al2024 nanocomposite can be attributed to the presence of very fine (<100 nm) particles of TiO_2 reinforcements.

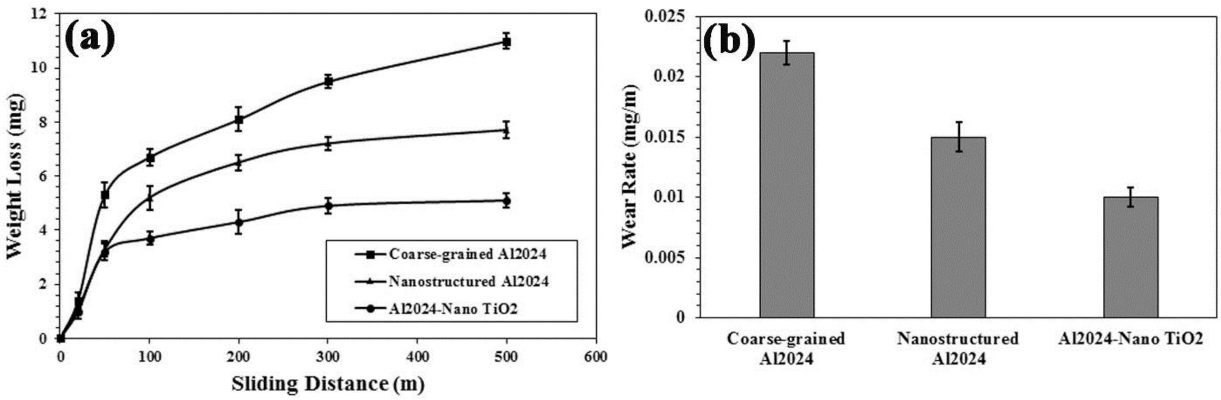

Fig. 6. (a) Wear mass loss of samples as a function of sliding distance and (b) wear rate of different samples.

Fig. 5. Bar chart showing the hardness value for the initial coarse-grained Al2024-T3 alloy, nanostructured Al2024 alloy, and Al2024-2wt.%TiO_2 nanocomposite prepared by MA and HP. To find the wear mechanisms of the samples; the worn surfaces and the wear debris were investigated by SEM. The SEM micrographs of the worn surfaces of the coarse-grained Al2024 alloy, nanostructured Al2024 alloy, and Al2024-2wt.% TiO_2 nanocomposite samples at 15 N applied normal load is presented in Fig. 7. The worn surface of the coarse-grained Al2024 alloy (Fig. 7a) was mostly covered with loose debris and delamination layers, indicating that adhesive wear and delamination were active for this sample. Some evidence of abrasive grooves were also observed on the wear track of this sample. SEM image of the wear track of the nanostructured Al2024 alloy (Fig. 7c) showed effects of plowed grooves, delamination layers, and craters, which are characteristics of abrasive, delamination, and adhesive wear. However, this sample showed less surface damage compared with the coarse-grained Al2024 alloy. The worn surface of the Al2024-2wt.%TiO_2 nanocomposite sample (Fig. 7e) mostly exhibited parallel grooves, indicating that the predominant wear mechanism was an abrasion. Some evidence of delamination and adhesive wear was also present on the worn surface. The Al2024-2wt.% TiO_2 nanocomposite had the lowest surface damage among the samples, which is consistent with its highest hardness value.

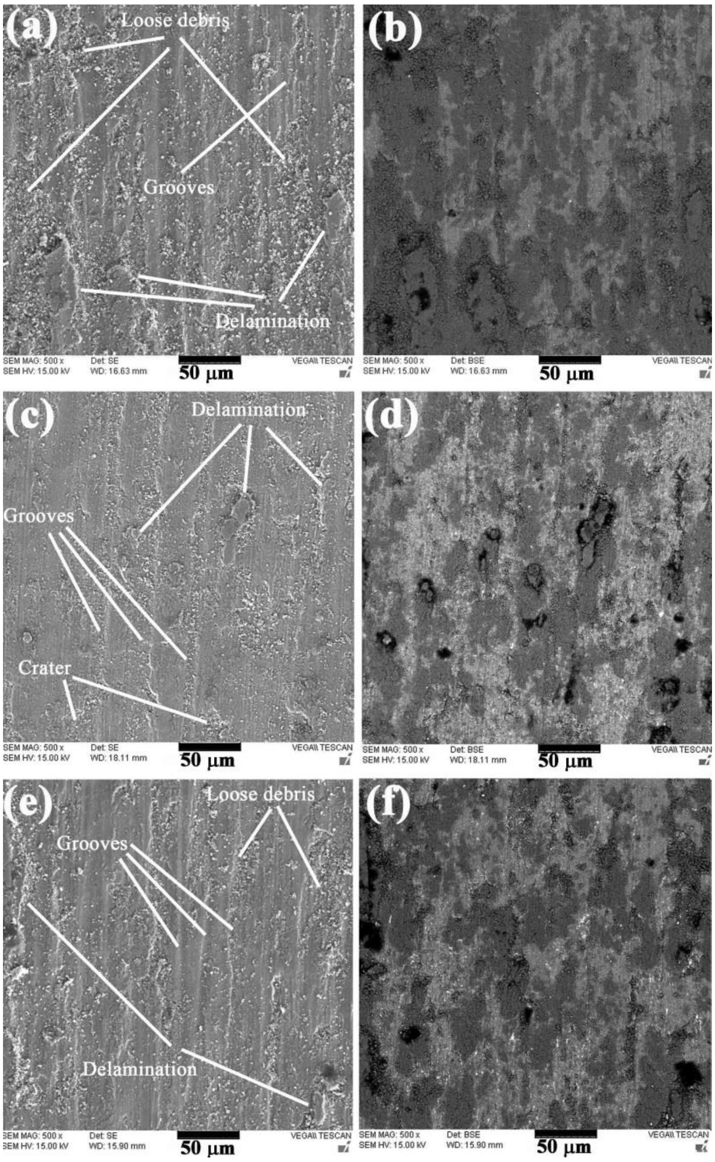

Fig. 7. SEM micrographs showing the worn surface of different samples, (a and b) coarse-grained Al2024 alloy, (c and d) nanostructured Al2024 alloy, (e and f) Al2024-2wt.% TiO_2 nanocomposite.

As can be seen in the backscattered SEM images in Fig. 7, most regions of all the worn surfaces were covered by a darker layer. A typical EDS analysis of the worn surface of the nanostructured Al2024 alloy is shown in Fig. 8. This EDS analysis showed that the darker areas in the worn surface contained a considerable amount of O and Fe (Fig. 8a). In contrast, EDS analysis of the bright areas showed the presence of a small amount of O and Fe. The presence of the higher amount of Fe in the darker layer implied the transfer of Fe from the steel pin to the worn surface, while the presence of O suggests the oxidation reaction. These results indicated that transfer and mechanical mixing of materials had taken place between the two sliding surfaces, and a mechanically mixed layer (MML) had been formed on the worn surface [22, 41]. Similar results were observed for other samples. As a result, it seems that a mechanical mixing/oxidation process was the controlling wear mechanism in the case of all samples.

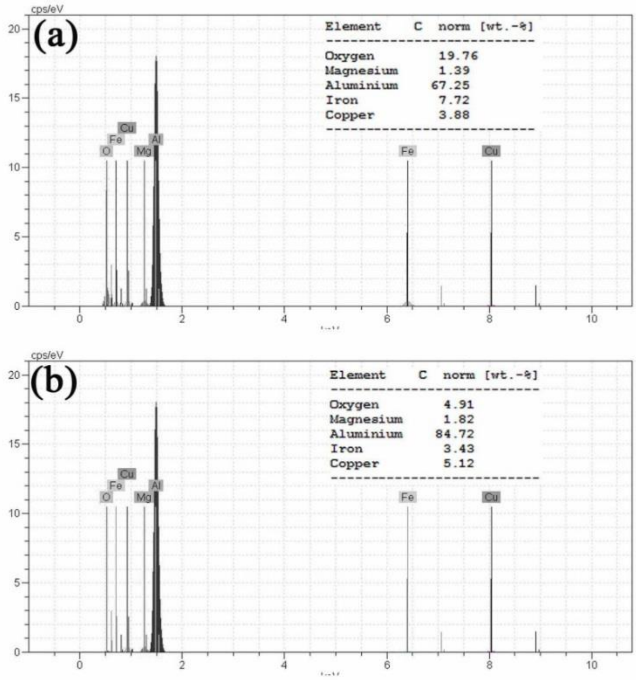

Fig. 8. Typical EDS analysis is taken from (a) dark areas and (b) bright areas of the worn surface of the nanostructured Al2024 sample.

Formation of MML on the worn surface of Al alloys and composites such as Al7075 alloy and Al-SiC composites [42], Al-Si [43], Al8090, and Al8090-SiC [44], Al6061, and Al-Mg-Si-CoNi [45] was also reported. Some characteristics of the MML are as follows [46, 47]: it has a darker color than other regions of the surface; it contains chemical elements like Fe coming from the counter body; contains oxides of Al and Fe, and has a higher hardness value than outside the MML. Because of its higher hardness, MML acts as a protective layer to the surface [41].

Fig. 9 shows the SEM images of wear products of different samples. A mixture of plate-like and fine wear debris was observed for the coarse-grained Al2024 alloy. Plate-like debris suggested delamination, while finer particles may be formed by abrasive or adhesive wear. For the nanostructured Al2024 alloy (Fig. 9b), a mixture of fine particles and small plate shape debris was present, suggesting abrasion and delamination. The wear debris of Al2024-2wt.% TiO_2 nanocomposite was in the form of very fine particles, indicating low surface damage for this sample. In fact, these fine particles were mostly removed from the grooves observed in Fig. 7e.

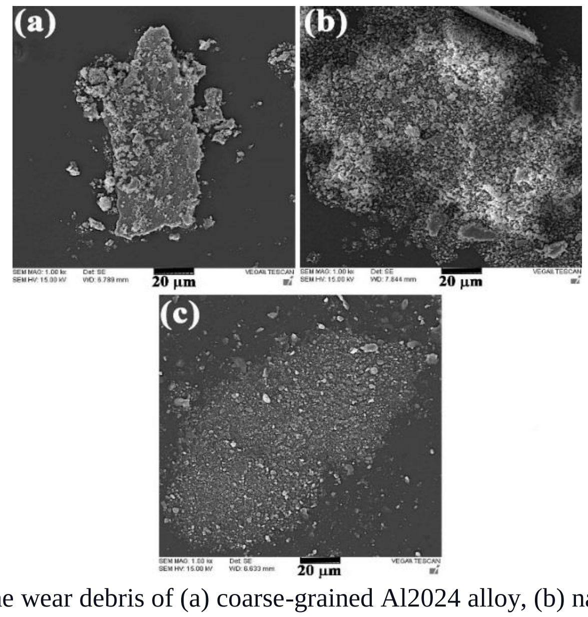

Fig. 9. SEM micrographs of the wear debris of (a) coarse-grained Al2024 alloy, (b) nanostructured Al2024 alloy, (c) Al2024-2wt.% TiO_2 nanocomposite.

The variation of friction coefficient of samples with sliding distance is shown in Fig. 10. In all samples, the friction coefficient gradually increased up to a sliding distance of 100 m to reach relatively steady values. The steady-state friction coefficient of coarse-grained Al2024 alloy, nanostructured Al2024 alloy, and Al2024-2wt.% TiO_2 nanocomposite varied between 0.25-0.5, 0.22-0.35 and 0.25-0.3, respectively. These results were in line with the previous reports of a decrease in friction coefficient with an increase in hardness [48], and were also in line with the wear rate results observed in Fig. 6. The presence of TiO_2 nanoparticles both decreases the average friction coefficient and its fluctuations. The decrease in the former is due to the decrease in metal-metal contact, as metal-ceramic contact has a lower friction coefficient than metal-metal contact. The decrease in the later can be attributed to the change in wear mechanism as it is well understood that the presence of hard ceramic particles decreases the adhesive wear in Al alloys [22, 49-51].

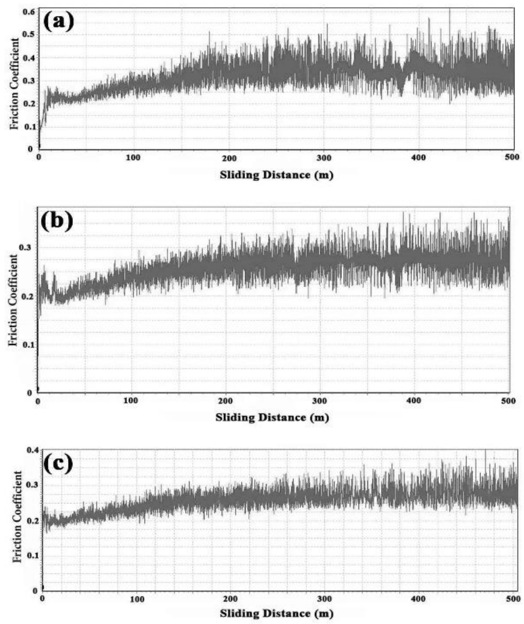

Fig. 10. Variation of friction coefficient with sliding distance, (a) coarse-grained Al2024 alloy, (b) nanostructured Al2024alloy, and (c) Al2024-2wt.% TiO_2 nanocomposite.

The friction coefficients obtained in the present study were in the range of those reported in the literature for nanostructured Al alloys and composites. Jafari et al. [52] observed an average friction coefficient of 0.3 for nanostructured Al2024 alloy. Mohammad Sharifi et al. [49] reported average friction coefficients of 0.3-0.4 for Al-B_4C nanocomposites containing 5-15 wt.% of B_4C particles. Hosseini et al. [53] observed friction coefficients between 0.3-0.6 for Al6061-3vol.% Al_2O_3 composites produced by MA and subsequent HP.

4. Conclusions

In this study, bulk nanostructured Al2024 alloy and Al2024-2wt.%TiO_2 nanocomposite were produced by MA and subsequent hot-pressing. Then, the density, hardness, and wear behavior of fabricated samples were evaluated. Based on the results obtained the following conclusions can be drawn:

1. The crystallite size of Al in both samples after MAand hot-pressing was less than 60 nm, and the Al lattice contained a high level of internal strain (> 0.5).

2. The hardness value of the nanostructured Al2024 alloy was ~ 198 HV, which is ~ 41% higher than that for the initial coarse-grained Al2024-T3 alloy (140 HV). The presence of the very fine and hard particles of TiO2 in the Al2024-2wt.%TiO_2 nanocomposite enhanced the hardness value to 238 HV.

3. The wear resistance of samples changes in the order of coarse-grained Al2024 alloy <nanostructured Al2024 alloy <Al2024-2wt.%TiO_2 nanocomposite, where the wear rate of the Al2024-2wt.%TiO_2 nanocomposite was ~ 0.66 of that for the nanostructured Al2024 alloy.

4. For all samples, the wear took place by a combination of abrasion, adhesion, and delamination mechanisms. However, the contribution of each mechanism was different. A mechanically mixed layer (MML) was formed on the worn surface of all samples. EDS analysis showed that this layer contains a considerable amount of Fe and O. Formation of this layer seems to be an important factor controlling the wear behavior of samples.

References

[1] M.T.A. El-Khair, A.A. Aal, "Erosion–corrosion and surface protection of a356 al/ZrO_2 composites produced by vortex and squeeze casting", Mater. Sci. Eng. A, Vol. 454-455, 2007, pp. 156-163.
[2] R. Ipek, "Adhesive wear behaviour of b_4c and SiC reinforced 4147 al matrix composites (al/B_4C–Al/SiC)", J. Mater. Proc. Technol., Vol. 162-163, 2005, pp. 71-75.
[3] K. Ozturk, R. Gecu, A. Karaaslan, "Microstructure, wear and corrosion characteristics of multiple-reinforced (SiC–B_4C–Al_2O_3) al matrix composites produced by liquid metal infiltration", Ceram. Int., Vol. 47, 2021, pp. 18274-18285.
[4] K.M. Shorowordi, A.S.M.A. Haseeb, J.P. Celis, "Tribo-surface characteristics of Al–Bb_4C and Al–SiC composites worn under different contact pressures", Wear, Vol. 261, 2006, pp. 634-641.
[5] S. Sharma, J. Singh, M.K. Gupta, M. Mia, S.P. Dwivedi, A. Saxena, S. Chattopadhyaya, R. Singh, D.Y. Pimenov, M.E. Korkmaz, "Investigation on mechanical, tribological and microstructural properties of Al–Mg–Si–T6/SiC/muscovite-hybrid metal-matrix composites for high strength applications", J. Mater. Res. Technol., Vol. 12, 2021, pp. 1564-1581.
[6] X.Z. Zhang, T.J. Chen, Y.H. Qin, "Effects of solution treatment on tensile properties and strengthening mechanisms of SiCp/6061Al composites fabricated by powder thixoforming", Mater. Des., Vol. 99, 2016, pp. 182-192.
[7] S.E. Hernández-Martínez, J.J. Cruz-Rivera, R. Martínez-Sánchez, C.G. Garay-Reyes, J.A. Muñoz-Bolaños, J.M. Cabrera, "Consolidation of AA 7075-2 wt% ZrO_2 composite powders by severe plastic deformation via ecap", Acta Metall. Sin. (Engl. Lett.), Vol. 29, 2016, pp. 895-901.
[8] X. Xie, S. Yin, R.N. Raoelison, C. Chen, C. Verdy, W. Li, G. Ji, Z. Ren, H. Liaoa, "Al matrix composites fabricated by solid-state cold spray deposition: A critical review", J. Mater. Sci. Technol., Vol. 86, 2021, pp. 20-55.
[9] B.A. Kumar, N. Murugan, I. Dinaharan, "Dry sliding wear behavior of stir cast AA6061-T6/AlNp composite", Trans. Nonferrous Met. Soc. China, Vol. 24, 2014, pp. 2785-2795.
[10] A. Mazahery, M.O. Shabani, "Microstructural and abrasive wear properties of SiC reinforced aluminum-based composite produced by compocasting", Trans. Nonferrous Met. Soc. China, Vol. 23, 2013, pp. 1905-1914.
[11] K.B. Lee, H.S. Sim, S.Y. Cho, H. Kwon, "Reaction products of Al–Mg/B4C composite fabricated by pressureless infiltration technique", Mater. Sci. Eng. A, Vol. 302, 2001, pp. 227-234.
[12] I. Kerti, F. Toptan, "Microstructural variations in cast B_4C-reinforced aluminum matrix composites.", Mater. Lett., Vol. 62, 2008, pp. 1215-1218.
[13] M. Kouzeli, C.S. Marchi, A. Mortensen, "Effect of reaction on the tensile behavior of infiltrated boron carbide–aluminum composites.", Mater. Sci. Eng. A, Vol. 337, 2002, pp. 264-273.
[14] R.M. Mohanty, K. Balasubramanian, S.K. Seshadri, "Boron carbide-reinforced alumnium 1100 matrix composites: Fabrication and properties", Mater. Sci. Eng. A, Vol. 498, 2008, pp. 42-52.
[15] I. Topcu, H.O. Gulsoy, N. Kadioglu, A.N. Gulluoglu, "Processing and mechanical properties of B_4C reinforced al matrix composites.", J. Alloy Cmpd., Vol. 482, 2009, pp. 516-521.
[16] M. Prashanth, R. Karunanithi, S. RasoolMohideen, S. Sivasankaran, "A comprehensive exploration on the development of nano Y_2O_3 dispersed in AA 7017 by mechanical alloying and hot-pressing technique", Ceram. Int., Vol. In Press, 2021, pp.
[17] E. Dastanpoor, M.H. Enayati, "Effect of milling intensity on mechanical alloying of Cu-Zr-Al system ", Ind. J Eng. Mater. Sci. , Vol. 22, 2015, pp. 521-526.
[18] C. Suryanarayana, "Mechanical alloying and milling", Progress in Materials Science, Vol. 46, 2001, pp. 1-184.
[19] C. Suryanarayana, N. Al-Aqeeli, "Mechanically alloyed nanocomposites", Prog. Mater. Sci., Vol. 58, 2013, pp. 383-502.
[20] J.N.R. Olveraa, G.J.G. Paredes, A.R. Serrano, E.R. López, E.M. Franco, P.T. Meza, L.D.B. Arceo, "Synthesis and characterization of a MoWC-Wc-NiC nanocomposite via mechanical alloying and sintering", Powder Technol., Vol. 271, 2015, pp. 292-300.
[21] R.M. Babaheydari, S.O. Mirabootalebi, G.H.A. Fakhrabadi, "Effect of alloying elements on hardness and electrical conductivity of Cu nanocomposites prepared by mechanical alloying", Iranian Journal of Materials Science and Engineering, Vol. 18, 2021, pp. 1-11.
[22] E.M. Sharifi, F. Karimzadeh, "Wear behavior of aluminum matrix hybrid nanocomposites fabricated by powder metallurgy", Wear, Vol. 271, 2011, pp. 1072-1079.
[23] M. Slimi, M. Azabou, L. Escoda, J.J. Suñol, M. Khitouni, "Structural and microstructural properties of nanocrystalline Cu–Fe–Ni powders produced by mechanical alloying", Powder Technol., Vol. 266, 2014, pp. 262-267.
[24] J.W. Kaczmar, K. Pietrzak, W. Wlosinski, "The

production and application of metal matrix composite materials", J. Mater. Process. Technol., Vol. 106, 2000, pp. 58-67.
[25] R. Karunanithi, S. Bera, K.S. Ghosh, "Electrochemical behaviour of TiO_2 reinforced Al 7075 composite", Mater. Sci. Eng. B, Vol. 190, 2014, pp. 133-143.
[26] C.A.V. Kumar, J.S. Rajadurai, "Influence of rutile (TiO_2) content on wear and microhardness characteristics of aluminium-based hybrid composites synthesized by powder metallurgy", Trans. Nonferrous Met. Soc. China, Vol. 26, 2016, pp. 63-73.
[27] S. Sivasankaran, K. Sivaprasad, R. Narayanasamy, V.K. Iyer, "Synthesis, structure and sinterability of 6061 AA_{100-x}–x wt.% TiO_2 composites prepared by high-energy ball milling", J. Alloy Cmpd., Vol. 491, 2010, pp. 712-721.
[28] S. Bera, S.G. Chowdhury, Y. Estrin, I. Manna, "Mechanical properties of Al7075 alloy with nano-ceramic oxide dispersion synthesized by mechanical milling and consolidated by equal channel angular pressing", J. Alloy Cmpd., Vol. 548, 2013, pp. 257-265.
[29] S.H. Nourbakhsh, M. Tavakoli, M.A. Shahrokhian, "Investigations of mchanical, mcrostructural and tibological properties of Al2024 nanocomposite reinforced by TiO_2 nanoparticles", Mater. Res. Express, Vol. 5, 2018, pp. 1-14.
[30] B. Prabhu, C. Suryanarayana, L. An, R. Vaidyanathan, "Synthesis and characterization of high volume fraction Al–Al_2O_3 nanocomposite powders by high-energy milling", Mater. Sci. Eng. A, Vol. 425, 2006, pp. 192-200.
[31] Z.R. Hesabi, H.R. Hafizpour, A. Simchi, "An investigation on the compressibility of aluminum/nano-alumina composite powder prepared by blending and mechanical milling", Mater. Sci. Eng. A, Vol. 454-455, 2007, pp. 89-98.
[32] E.M. Ruiz-Navas, J.B. Fogagnolo, F. Velasco, J.M. Ruiz-Prieto, L. Froyen, "One step production of aluminium matrix composite powders by mechanical alloying", Composites, Vol. 37, 2006, pp. 2114-2120.
[33] Y. Saberi, S.M. Zebarjad, G.H. Akbari, "On the role of nano-size SiC on lattice strain and grain size of Al/SiC nanocomposite", J. Alloy Cmpd., Vol. 484, 2009, pp. 637-640.
[34] I. Ozdemir, S. Ahrens, S. Mucklich, B. Wielage, "Nanocrystalline Al–Al_2O_3p and SiCp composites produced by high-energy ball milling", J. Mater. Proc. Technol., Vol. 205, 2008, pp. 111-118.
[35] K. Williamson, W.H. Hall, "X-ray line broadening from field aluminum and wolfram ", Acta Metallurgica, Vol. 1, 1953, pp. 22-31.
[36] Handbook Comittee, "Standard test method for wear testing with a pin-on-disk apparatus", ASTM, 2005.
[37] H. Ashrafi, M.H. Enayati, R. Emadi, "Nanocrystalline Al/Al_{12}(Fe,V)$_3$Si alloy prepared by mechanical alloying: Synthesis and thermodynamic analysis", Adv. Powder Technol., Vol. 25, 2014, pp. 1483-1491.
[38] N. Yazdian, F. Karimzadeh, M. Tavoosi, "Microstructural evolution of nanostructure 7075 aluminum alloy during isothermal annealing", J. Alloy Cmpd., Vol. 493, 2010, pp. 137-141.
[39] M. Jafari, M.H. Abbasi, M.H. Enayati, F. Karimzadeh, "Mechanical properties of nanostructured Al2024–MWCNT composite prepared by optimized mechanical milling and hot pressing methods," Adv. Powder Technol., Vol. 23, 2012, pp. 205-210.
[40] G.E. Dieter, Mechanical metallurgy, ed., McGraw-Hill, Singapor, 1988, 215.
[41] M.J. Ghazali, W.M. Rainforth, M.Z. Omar, "A comparative study of mechanically mixed layers (mmls) characteristics of commercial aluminium alloys sliding against alumina and steel sliders", J. Mater. Proc. Technol., Vol. 201, 2008, pp. 662-668.
[42] B. Venkataraman, G. Sundararajan, "Correlation between the characteristics of the mechanically mixed layer and wear behaviour of aluminium, Al-7075 alloy and Al-MMCs", Wear, Vol. 245, 2000, pp. 22-38.
[43] X.Y. Li, K.N. Tandon, "Microstructural characterization of mechanically mixed layer and wear debris in sliding wear of an Al alloy and an Al based composite", Wear, Vol. 245, 2000, pp. 148-161.
[44] J. Rodríguez, P. Poza, M.A. Garrido, A. Rico, "Dry sliding wear behaviour of aluminium–lithium alloys reinforced with SiC particles", Wear, Vol. 262, 2007, pp. 292-300.
[45] H.J. Kim, J.M. Lee, Y.H. Cho, S.Y. Sung, B.S. Han, Y.S. Ahn, "Microstructures and wear properties of Al–Mg–Si alloy with the addition of ball-milled CoNi powders", Mater. Charact., Vol. 70, 2012, pp. 137-144.
[46] M.R. Rosenberger, C.E. Schvezov, E. Forlerer, "Wear of different aluminum matrix composites under conditions that generate a mechanically mixed layer", Wear, Vol. 259, 2005, pp. 590-601.
[47] H. Ashrafi, M.H. Enayati, R. Emadi, "Tribological properties of nanostructured Al/Al_{12}(Fe,V)$_3$Si alloys", Acta Metall. Sin. (Engl. Lett.), Vol. 28, 2015, pp. 83-92.
[48] A.S. Anasyida, A.R. Daud, M.J. Ghazali, "Dry sliding wear behaviour of Al–12Si–4Mg alloy with cerium addition", Mater. Des., Vol. 31, 2010, pp. 365-374.

[49] E.M. Sharifi, F. Karimzadeh, M.H. Enayati, "Fabrication and evaluation of mechanical and tribological properties of boron carbide reinforced aluminum matrix nanocomposites", Mater. Des., Vol. 32, 2011, pp. 3263-3271.

[50] K. Kato, "Wear in relation to friction — a review", wear, Vol. 241, 2000, pp. 151-157.

[51] F. Tang, X. Wu, S. Ge, J. Ye, H. Zhu, M. Hagiwara, J.M. Schoenung, "Dry sliding friction and wear properties of B_4C particulate-reinforced Al-5083 matrix composites", wear, Vol. 264, 2008, pp. 555-561.

[52] M. Jafari, M.H. Enayati, M.H. Abbasi, F. Karimzadeh, "Compressive and wear behaviors of bulk nanostructured Al2024 alloy", Mater. Des., Vol. 31, 2010, pp. 663-669.

[53] N. Hosseini, F. Karimzadeh, M.H. Abbasi, M.H. Enayati, "Tribological properties of Al6061–Al_2O_3 nanocomposite prepared by milling and hot pressing", Mater. Des., Vol. 31, 2010, pp. 4777-4785.

.